Journal of Research in Chemistry

E-ISSN: 2709-9423
P-ISSN: 2709-9415
JRC 2022; 3(1): 34-46

www.chemistryjournal.net
Received: 15-01-2022
Accepted: 18-03-2022

Shruti Verma
Research Scholar,
Department of Science,
Faculty of Chemistry,
Malwanchal University,
Indore, Madhya Pradesh,
India

Correspondence
Shruti Verma
Research Scholar,
Department of Science,
Faculty of Chemistry,
Malwanchal University,
Indore, Madhya Pradesh,
India

An analysis the techniques of non-destructive holography for different structures

Shruti Verma

Abstract
"Non-Destructive Testing" refers to any method used to assess performance without harming the test object (NDT). Over the past quarter century, NDT has undergone unprecedented development and expansion. In terms of originality and progress, it is now considered to be among the most rapidly expanding technologies available. Holographic techniques were used in the continuing design, engineering, and testing of the assemblies shown, and they have shown to be the most efficient way to assess their crucial dynamic properties. The objectives of this study the methods of non-destructive holography for different structures. The basic idea behind holographic non-destructive testing is well known: the component being tested is exposed to a mechanical condition of stress that is equally distributed throughout its surface.

Keywords: Non-destructive testing, holographic, interferometry, dynamic structure, digital, optic

Introduction
Non-Destructive Testing (NDT) refers to any inspection, test, or assessment that is conducted on a test item without causing any damage to the thing in order to identify the existence or absence of conditions or discontinuities that might compromise the object's utility or serviceability. Other properties of the test object, such as size, dimension, configuration, or structure (alloy content, hardness, grain size, etc.), can be measured using nondestructive testing. The most basic definition is an analysis done on an object of any size, shape, or substance to check for flaws and other defects, or to assess its overall quality. Similar terms, such as non-destructive inspection (NDI) and non-destructive evaluation (NDE), are also often used to refer to this method. Buildings, planes, and consumer goods may all seem infallible because of this technology, yet the typical individual has no idea it exists. It is true that NDT cannot ensure that failures will never occur, but it does play a crucial part in doing so. Even if NDT is performed correctly, other factors, such as poor design or inappropriate use, might still play a role in the failure.

Methods of non-destructive holographic interferometry for the dynamic structural
Holographic interferometry has been used to successfully describe the composition and behaviour of several kinds of stressed structures. These holographic programmes provide some of the best modal and dynamic analysis techniques currently on the market. Without inflicting any damage, the system detects and displays the vibrational modes, displacements, and motion geometry in real time. Studies of structures and processed materials are possible with very small amplitude stimulation, and the generated data may be used to improve the accuracy of mathematically derived structural models. Holographic interferometry is an effective resource for the initial design and development of novel materials like graphite-epoxy fibre reinforced polymer matrix composites. This sort of material is being used more frequently in high-tech aerodynamic, automotive, and other highly mobile systems. These manifestations are indicative of a wide variety of structural stresses, including mechanical, thermal, and acoustic, that are caused by irregularities and defects that are otherwise hidden. Having this kind of information is often crucial for making decisions about mechanical configurations and designs, as well as operating conditions, for structures composed of complex manufactured materials.

Methods

Holographic interferometry has a number of mature and well-established applications in several facets of structural research. New technological advancements in laser and holographic instruments have also significantly increased the value and utility of these analytical tools. Holography techniques known as "real-time" and "Multi-exposure" are the topics of this debate. The first phrase describes the superposition of an object's hologram over the actual thing when it is under a slight stress. This is done in order to see how small displacement variations impact the object's structure while stress is applied in real time. The second phrase refers to a pair of holograms that are often produced when the item being studied experiences some sort of differential stress in between exposures. Aspects of the geometry and size of stress-induced displacements in a structure are revealed by both procedures. Metal and epoxy-matrix composite substrates are two examples of advanced material architectures that lend themselves nicely to this sort of testing. Very small strains and displacements can be induced in structures by applying mild mechanical, thermal, or acoustic stress without jeopardising the integrity of the structures. We then employ holographic techniques to inspect the structure and materials for any defects. A simplified diagram of the holographic system employed in this study is presented in Figure 1. The system includes a single-frequency, single-mode Argon-ion laser. "Instant holocameras" built of photo-thermoplastic were used to record holograms. Imagery of the holograms was recorded using a high-definition television camera and screen. Holograms at a wavelength of.5145 microns were made with controlled exposures to produce the high contrast ratios desired in the interferograms. A holographic plate was illuminated by a reference beam, while the object beam was directed towards the structure of interest. A hologram of the assembled composite structure might be taken at this setup in either real time or with several exposures. Holographic techniques were used for the purpose of studying the composition, behaviour, and mounting geometry of a graphite-epoxy composite part used in an experiment.

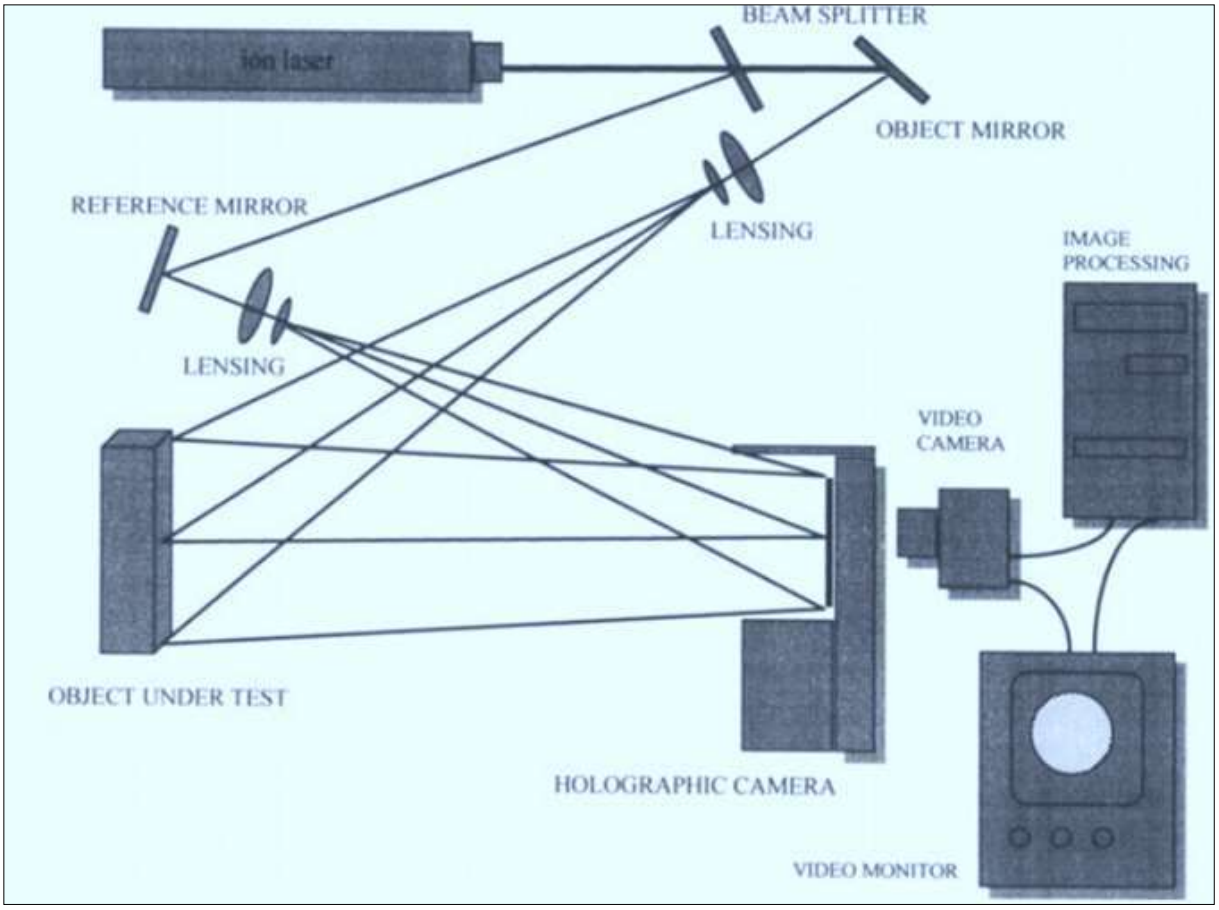

Fig 1: Holographic interferometry system.

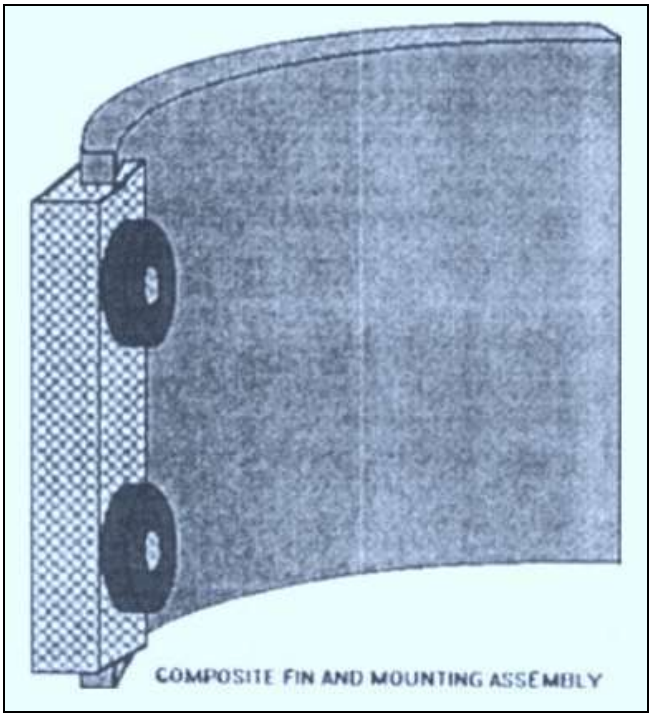

Fig 2: Graphite-epoxy composite structure assembly configuration.

Holograms of the displacement patterns of created stress are used to precisely map the location and extent of nonuniformities, discontinuities, microcracks, and other structural faults in the volume and mounting of the composite material. These "roadmaps" may be compared to the requirements of the testing and production settings. This allows the optimal design, engineering, and most importantly, operational inspection to be determined based on the structure's real-world behaviour. The data obtained represent an assembly of a composite structure made from a polymer matrix. Mass loading, composite thickness, shape, as well as material density, homogeneity, and constraint, all have significant impacts on the resulting fringe patterns. We may expect the holographic fringes to clearly display any flaws, imperfections, or inconsistencies in the structural volume of the material.

Procedure

When the test composite structure assembly was placed and in a "undisturbed" state, a holographic exposure was made (isolated from any induced vibrations or stresses). The resulting real-time holographic picture that was overlaid was then shown on the monitor. As the composite structural assembly was strained, the interference fringes that were created mapped the displacements and geometries. The holographic pictures are examined in real-time while the fringe patterns are tuned to prevent rigid body motion, and the outcomes are recorded (imaged) in the areas of greatest significance. The whole motion geometries of the generated stresses in the assemblies may be precisely described by recording multi-exposure holograms that trace the distinct "before and after" behaviour. The holographic fringes' displacements' size is very tiny, making them nondestructive to the assembly being tested. Each fringe represents an isobar of displacement of one-half wavelength of the illuminating light in the real-time and multi-exposure holographic image. The displacement that results from this is 0.2573 microns (10.1 micro-inches).

Results

Primary fringe maps similar to those in Figure 3 are presented by the simplest holographic stress analysis of a homogenous, symmetrically placed composite structural assembly. These images depict holograms of the composite structure's highly strong simple bending and torsional geometries. The mechanically generated stresses resulting in these fringe patterns were created by the application of a very low intensity uniform force. There are no obvious structural flaws that might also cause the fringes to be warped or altered by constraints or mass loading effects. The bending of the structure is defined as a displacement phenomenon whose amplitude grows linearly from the mounting assembly of the component by the holographic fringe pattern seen in the first image. The second figure's fringe geometry shows a significant pattern of torsional displacement coupled with restraint at the mounting of the assembly.

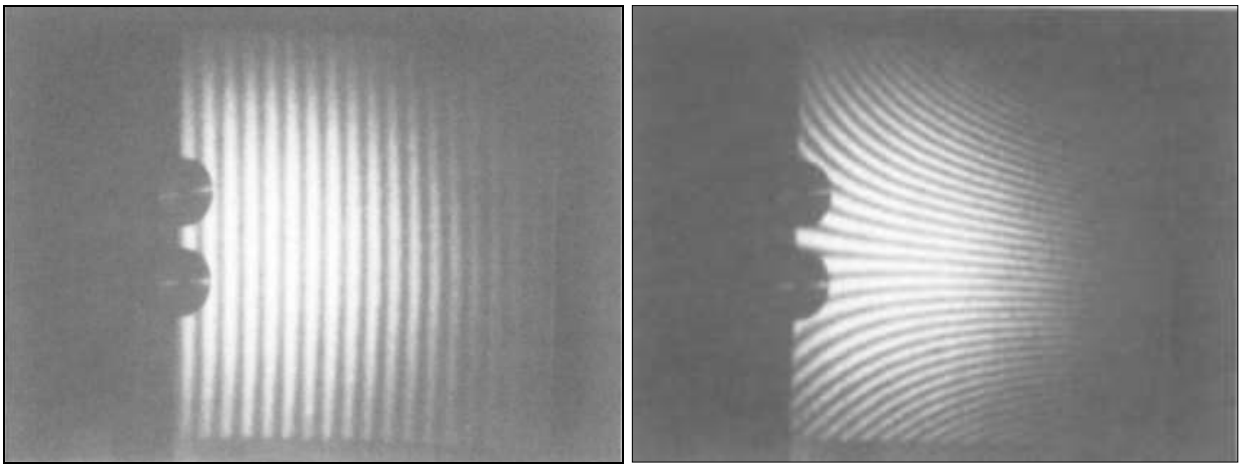

Fig 3: Fringe patterns showing simple bending and torsional geometries

The effects of additional stress are illustrated in Figure 4. As displacement varies throughout the surface as a function of localised stress in the substrate, fringe geometries become increasingly complicated. It should be noted that mounting and material abnormalities can potentially alter this type of geometry. Changes in the substrate can also selectively alter bending and torsion patterns. Holograms with fundamental fringe geometries that have been altered by nonisotropic

mounting limitations are seen in Figure 5. The distortion describes how the structure is affected by non-uniform restraint and loading. The basic bending geometry in the first picture is mapped by a real-time hologram that depicts a strong stress gradient. Extreme restraint on the mounting assembly and significant displacements brought on by the component's free edge's direct mechanical stress may cause aberrant behaviour or even component breakdown.

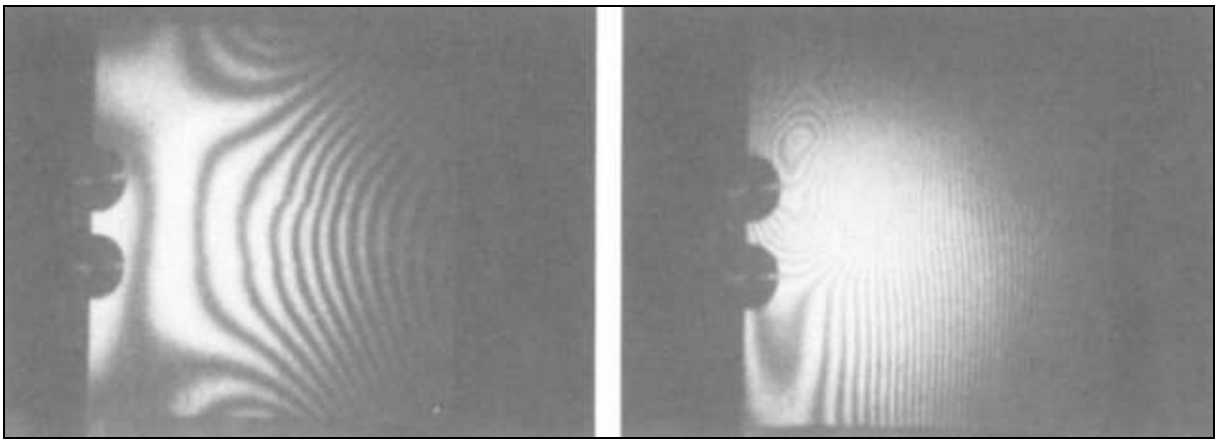

Fig 4: Holograms showing high stress gradient and differential loading effects.

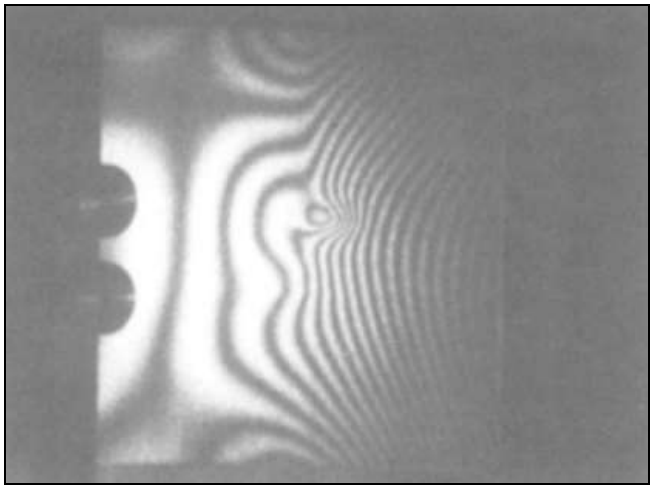

Fig 5: Included structural flaw.

In the second example, we see a hologram with a fringe pattern that is characteristic of a very different loading situation from the one used to create the first. Stress is concentrated in the mounting area, as demonstrated by the circular fringes, which contrast dramatically with the lack of surrounding fringe continuity. There is more evidence that a restriction or aberrant mass loading is at play here. A catastrophic breakdown of a crucial component may follow from these actions.In Figure 5, we see a hologram of the composite part with the thermal stress artificially lowered. Fringe pattern distortions reveal budged imperfections in the composite substrate. This irregularity, although physically present in the composite, manifests as a topographical offset on the substrate. When these defects manifest as inclusions, trapped gas, delaminations, or anything else associated with the manufacturing process, they are easy to spot. Testing and adjusting the parts and, eventually, the production process might limit the occurrence of such material-related irregularities. Final structural analysis and development requires a direct comparison between the composite structure assembly's real configuration and the relevant displacement maps of the entire system of which it is a part. This comparison illustrates how the operational environment may really affect the complete mechanical system. Mechanical stability ensures that the assembly's components are stressed as little as possible when in use.

NDT of composite plates by holographic Vibrometry

Laminate composites and sandwich materials may be examined by using lamb waves, which interact with delaminations. Non-contact detection of Lamb waves induced in a structure was made possible with the introduction of scanning laser Doppler interferometric techniques. It was demonstrated that by utilising the local vibrational difference between a delaminated patch and the surrounding structure, defect maps could be created. To highlight local damage differences, time-domain laser Doppler measurements analysis techniques were developed. Among these, calculation of the local energy from temporal wave fields and spatial and temporal discrete Fourier transforms methods have demonstrated their effectiveness. However, scanning laser Doppler vibrometry is a time-consuming method that prevents real-time observations with great spatial resolution.

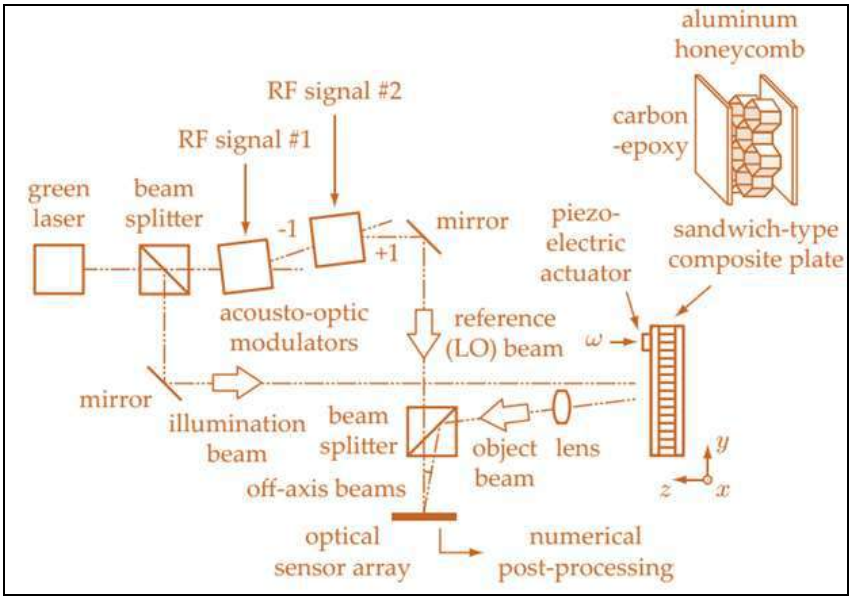

Fig 6: Mach-Zehnder optical holographic interferometer

Separating the main laser beam into two channels allows for greater flexibility. When the object is vibrating at an angular frequency of, the optical field is backscattered by it in the object channel, resulting in two modulation sidebands at small vibration amplitudes. As a result of two acousto-optic modulators, the frequency of the optical field in the reference channel may be changed. When the two optical beams collide, an interference pattern is produced, which is recorded by the camera's sensor array. Holographic rendering is a popular method for creating 3D visuals, and it often involves a mathematical formula to produce the final product. Fresnel lens transformation**.** The composite is a symmetric sandwich with 3/8"-thick aluminium honeycomb cells that are 2.5 cm thick. The skin is an epoxy resin-coated stack of woven carbon fibre plies measuring 1.1 mm thick and having a density of 1.7 g/cm^3. The semi-analytical finite element (SAFE) approach is utilised to determine the dispersion relation of the first antisymmetric Lamb mode A0 using its standard mechanical characteristics, presented in Tab. I for one woven ply. Fig. 7 displays the plot of this dispersion relation. To cause a small-scale, imperceptible separation of the skin from the honeycomb, the composite was struck at 1 J on the monitoring side. A piezoelectric transducer was attached to the carbon/epoxy plate, as illustrated at the bottom of Fig. 8, in order to produce steady-state Lamb waves in the plate (a). A sinusoidal signal with a sweeping angular frequency ω is applied to the piezo disc, which has a 2 cm diameter. Holographic vibrometry uses resonant Lamb waves as a monitoring targe.

$$C = \begin{pmatrix} 60 & 15 & 7 & 0 & 0 & 0 \\ & 60 & 7 & 0 & 0 & 0 \\ & & 14 & 0 & 0 & 0 \\ & & & 4 & 0 & 0 \\ & \text{sym.} & & & 4 & 0 \\ & & & & & 7 \end{pmatrix}$$

Fig 7: Stiffness tensor components Cij of the composite material, in GPa. Plies are stacked along the out-of-plane direction z.

By assuming a circular defect geometry, we are able to quantify the local delamination defect and demonstrate how altering the boundary conditions in the carbon fibre epoxy plate generates local resonances of anti-symmetric Lamb waves at low frequencies that are proportional to the defect size. Kinematics of flexural A0 Lamb waves in an isotropic plate are described by the Kirchhoff-Love equation.

$$\frac{\partial^2 z}{\partial t^2} + \frac{Eh^2}{12\rho\left(1-\nu^2\right)}\nabla^4 z = 0$$

where z is the out-of-plane motion, ∇ is the gradient operator, h is the thickness of the plate, E is the young modulus of the material, ρ its density, and ν its Poisson's ratio. In polar coordinates (r, θ), the harmonic solutions of eq.1 take the form z = Z (r, θ) exp(iωt), where i is the imaginary unit.

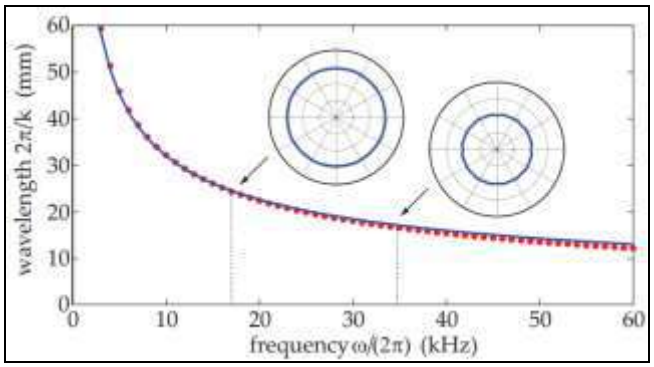

Fig 8: Dispersion relation of the first antisymmetric Lamb mode (A0) in a 1.1 mm-thick carbon fiber epoxy plate

The SAFE technique is used to numerically resolve the Rayleigh Lamb equation, resulting in the dots. In the low frequency approximation for a homogeneous and isotropic plate, the statement of the Rayleigh-Lamb equation looks like this: Eq. hk ≪ 1 (where h is the thickness of the plate and k is the wave vector) corresponds to the line (2). Lamb mode slowness curves at 17 kHz and 34.5 kHz were computed.

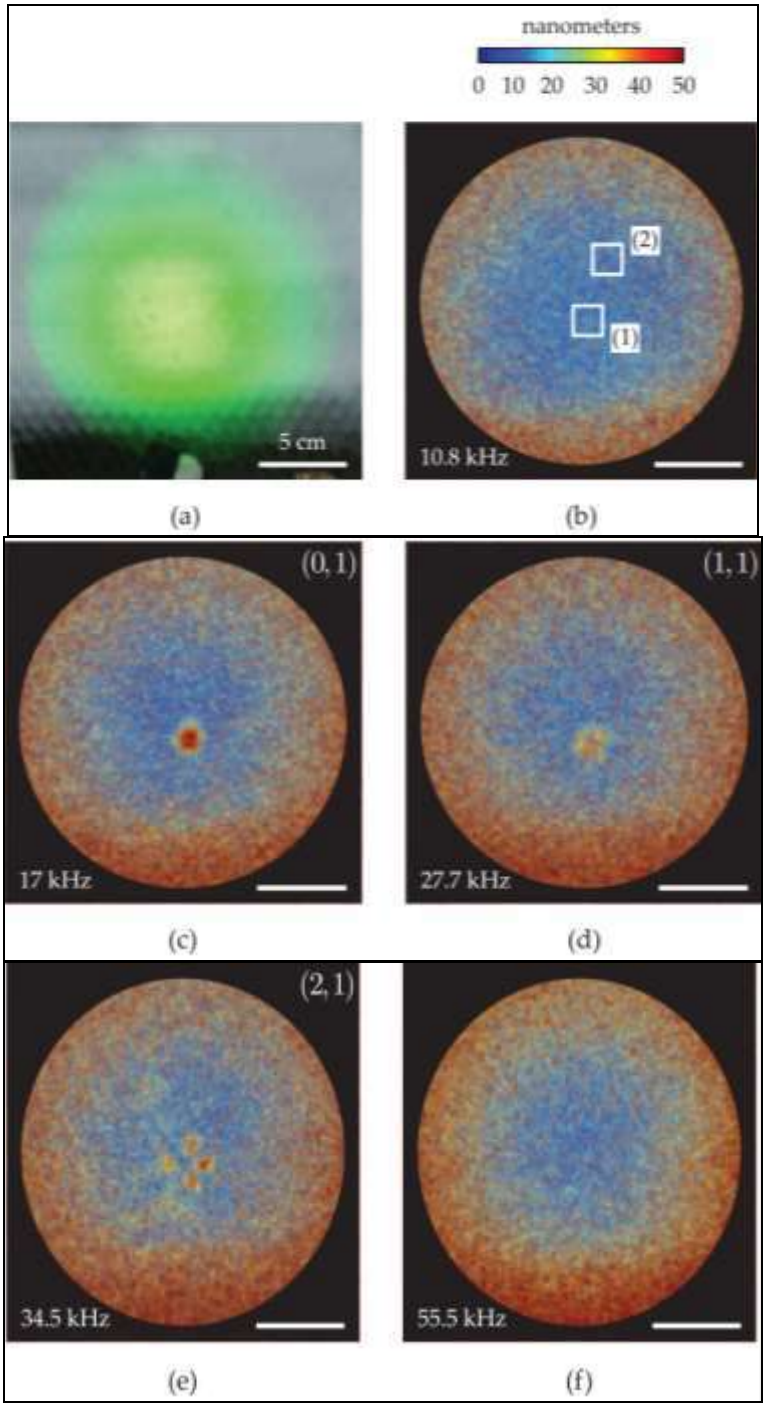

Fig 9: Direct image of the composite plate used for the experiment, illuminated with the green laser (a). Holographic images of the out-of-plane vibration (b-f). Geometric vibration modes : (m, n) = (0, 1) at 17 kHz (c), (m, n) = (1, 1) at 27.7 kHz (d), (m, n) = (2, 1) at 34.5 kHz (e). Zone (1) corresponds to the delamination region, and zone (2) is a healthy region, 5 cm away from zone (1).

The Rayleigh-Lamb dispersion relation of the A0 mode in the low frequency approximation is introduced to derive the steady-state solutions Z(r, θ)

$$\omega = \frac{1}{\sqrt{12}} k^2 c_p h$$

where k is the wave vector and cp = p E/ρ (1 − ν 2) is the speed at which longitudinal waves spread out on an isotropically thin plate. Because our material is anisotropic, the cp we have calculated cannot be used in this context. However, we demonstrate that the composite may be assumed to be a quasi-isotropic ply throughout the monitored frequency range, from 10 kHz to 60 kHz, for which cp can be evaluated by a fitting technique of dispersion relationships. The mechanical parameters of the plate were used to derive the slowness curves for the Lamb modes at 17 kHz and 34.5 kHz (stiffness tensor, thickness, angles between woven plies). The polar curves given in Fig. 4.8 suggest that the material exhibits quasi-isotropic behaviour at these frequencies. After obtaining the values of the mechanical parameters, we fit the dispersion relation determined using the SAFE technique and reported in Fig. 2 (dots) with Eq.2. This yields an equivalent velocity of cp = 5150 m/s (plotted as a line).

Figure 9 is a holographic representation of the amplitude of the out-of-plane vibration at various frequencies.

Narrowband detection's frequency was scanned between 10 and 60 kHz so that vibrations could be tracked. Each photograph took half a second to capture completely. The delamination defect's vibration modes were assumed visually to be Fig. 9(c) corresponding to the mode (m, n) = (0, 1), (ii) Fig9(d) corresponding to the mode (m, n) = (1, 1), and (iii) Fig. 4.9(e) corresponding to the mode (m, n) = (0, 1). (2, 1). In Fig. 9(b), we can see that two distinct sections, (1) in the delamination zone and (2) in a typically healthy part, have been marked off. Spectral vibration amplitudes are compared between the two regions in Fig. 10. We estimated the radius an of the damaged region using the resonance frequencies of the geometrical modes (0,1), (1,1), and (2,1), as given by Eq. 5. With the use of the given values for h and cp, we were able to calculate the values for a01, a11, and a21. These radii are all around the same size. We examined the lateral extension of the vibrating zone for the mode (m, n) = (0, 1) and the mode (m, n) = (2, 1), which demonstrate a strong signal-to-noise ratio, to verify this theoretical approach to delamination vibrations (Fig. 4). Images of the observed local out-of-plane amplitude (a) and the simulated solutions of the steady-state modes Z (b) for eigenvalues γ01 (c) & γ21 (d) were given in Figure 5.

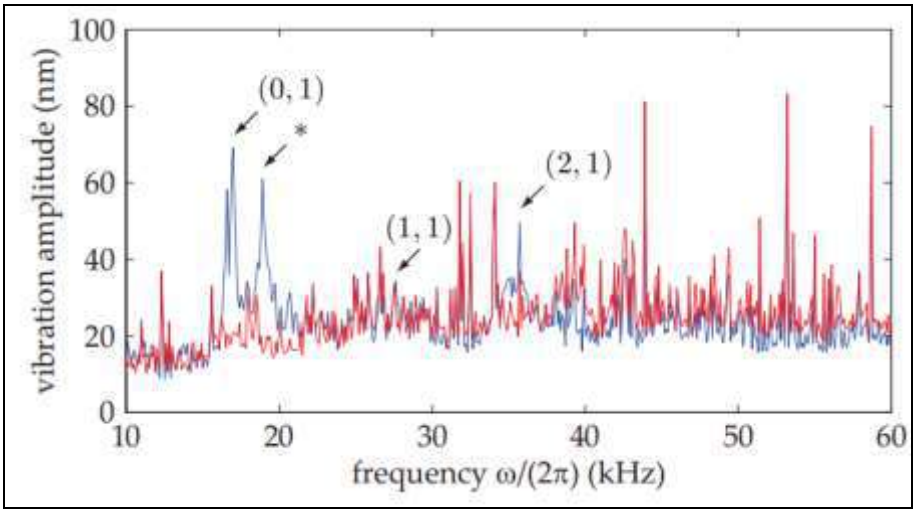

Fig 10: Local out-of-plane vibration amplitude versus excitation (and measurement) frequency ω/(2π) in the delamination region of the composite plate (blue line, region (1)), and 5 cm away from the region (red line, region (2)). Specific resonances of the delamination region corresponding to the spatial vibration modes (m, n) = (0, 1), (m, n) = (1, 1), and (m, n) = (2, 1) are highlighted by arrows.

The peak highlighted by ∗ is an alternate (m, n) = (0, 1) mode assumed to be caused either by (i) anisotropy in the carbon epoxy plate and/or (ii) non-circular symmetry of the delamination defect.

Both coefficients Am and Cm for each mode were estimated using the boundary condition Z(amn) = 0 and the maximum amplitude measured on the experimental data. Figures 11(e) and (f) compare calculated and measured vibration amplitude profiles and demonstrate good agreement for both. In order to identify delamination defects in sandwich-type composite plates, we have established a wide-field, real-time structural health monitoring approach. Low frequency flexural waves were generated in the plate with the assistance of an ultrasonic actuator, and time-averaged heterodyne holography and a dual local oscillator were used to take non-contact vibrometric measurements.

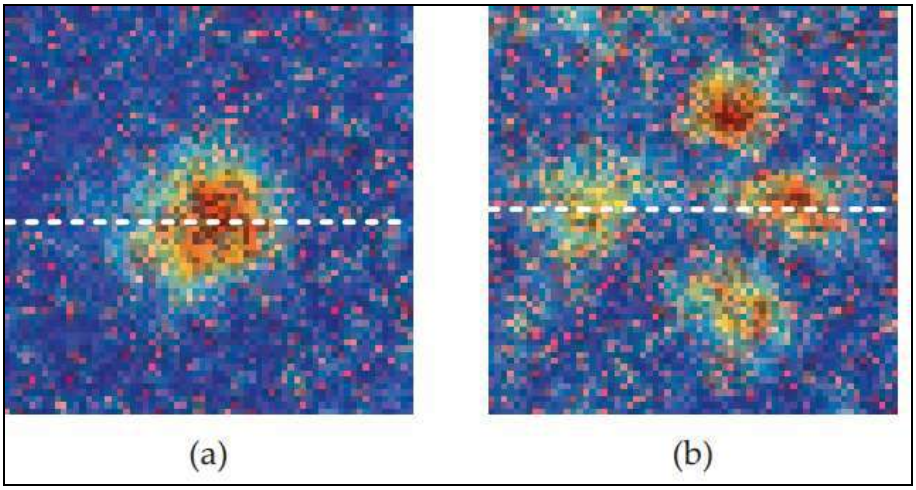

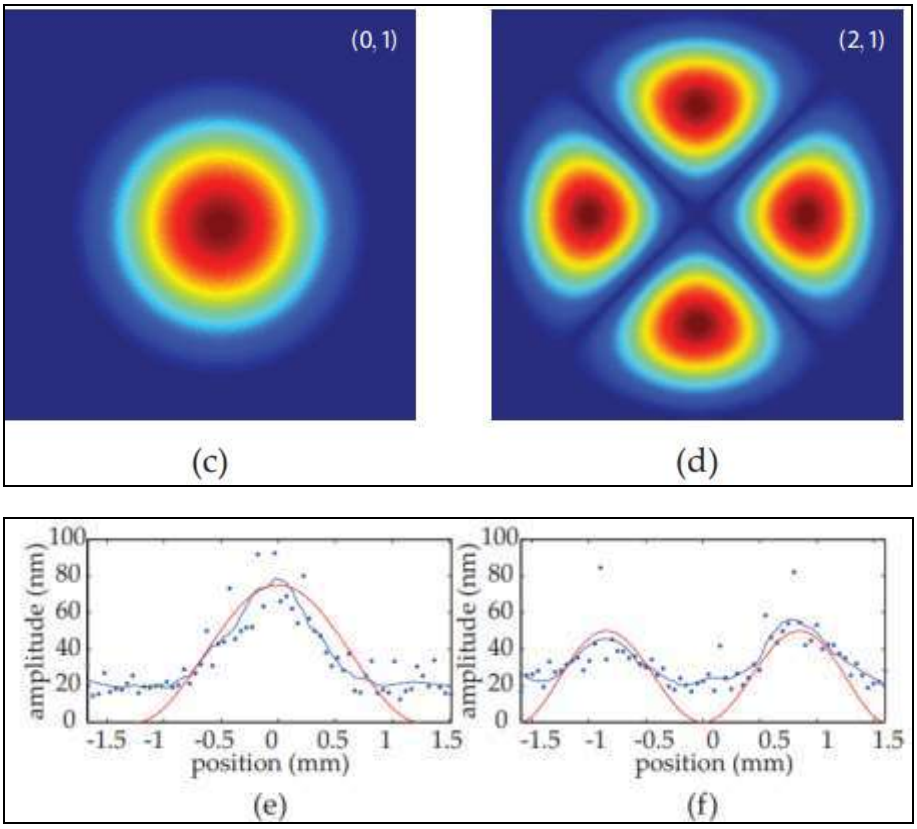

Fig 11: Lateral extension of the vibrating region for the spatial vibration modes (m, n) = (0, 1) at 17 kHz and (m, n) = (2, 1) at 34.5 kHz. Holographic images of experimental results (a,b). Calculated modes (c,d). Profile of the out-of-plane amplitude along a line (e,f); blue : experiments, red : theoretical curve.

Two optical modulation sidebands were sampled and utilised to calculate the amount of camera bandwidth vibration. At the frequency of the stimulation, it was found that flexural waves and delamination flaws in a sandwich composite plate with an aluminium honeycomb core were connected. Sweeping the excitation and detection frequencies allowed for the measurement of the vibration spectra in close proximity to and far away from the problem. Low-frequency resonances were seen locally in a composite plate, and the likely cause was the presence of local delaminations. The visible layer's mechanical characteristics and the flexural wave's first resonance frequency were used to determine the defect's magnitude. There is great agreement between the results of experimental study on the vibration frequency of a local delamination of the composite and its lateral expansion and the suggested analytical connection.

Application of digital holography for nde of metallic tubes

Digital holography has shown to be a powerful online inspection tool for non-destructive testing in a variety of scientific and technical disciplines. These include fluid mechanics, microscopy, profile measuring, 3D object recognition, deformation measurement, and vibration analysis. This method of holography typically entails capturing an optical field emanating from a lit object in a diffraction plane and numerically estimating the dispersion of the optical wave field in the reconstruction plane. During the process of numerical reconstruction, the digitally sampled hologram may be utilised to ascertain not only the intensity but also the phase information of the recorded wavefield. One of the most significant applications of digital holography is holographic interferometry, which is related to Holographic Non-Destructive Testing (HNDT). In HNDT, a very little tension or excitation is applied to the specimen via holographic interferometry. Measure the mechanical and thermal response of a component to its design environment using HNDT for a rapid, low-cost option to back up your design or simulation. Holographic nondestructive testing may detect and see micrometer-scale deformations through the use of fringe patterns. Artificial flaws in the material manifest as a visual inhomogeneity in the fringe pattern, which is a direct result of the surface's distortion.

Digital holographic recording and Reconstruction

In holography the entire optical wave field is recorded by coding the information with the help of a reference wave which is mutually coherent with the object wave field. The object wave field UO (x, y) scattered by the specimen to be evaluated is superposed to the reference wave field UR (x, y). The resulting intensity distribution H (x, y) recorded by the CCD/CMOS target is written as

$$H=|U_r+U_o|^2=|U_r|^2+|U_o|^2+U_r^*U_o+U_rU_o^* \quad (1)$$

Here '*' denotes complex conjugation and the spatial (x, y) coordinates are omitted for clarity. Equation [1] constitutes what is classically called the digital hologram. It includes three orders: the 0-order is composed of terms $|U_r + U_0|^2$ commonly referred as DC; the +1 order is the term U_r*U_0 and the −1 order term U_rU_0 *is denoted as the twin image. Further optical reconstruction of the wave field is done numerically by pointwise multiplication of the recorded

hologram data with a numerical model of the reference wave and propagation of the resulting complex field.

$$H.U_r=(|U_r|^2+|U_o|^2)U_r+U_o^* U_r^2+|U_r|^2U_o \quad (2)$$

The Fresnel-Kirchoff integral, which is derived from the Fourier transform of the product of the transmittance and the quadratic phase factor, is used in the numerical reconstruction process to represent the complex amplitude of the diffracted wave field at the real picture plane. The intensity of the actual picture is determined by the complex amplitude's resultant modulus.

Schematics of the holographic interferometer's optics

Digital holograms are made by interferometrically mixing two waves, one representing the reference object and the other representing the item of interest, at the surface of a pixel matrix image sensor device (CCD/CMOS camera). The resulting holographic interference patterns are digitally sampled and stored by a CCD/CMOS camera, and the computer then utilises those samples to numerically reconstruct the image. Targeted by a sensor, the light field's amplitude and phase distributions are recorded as a microscopic interference pattern. Light grains and micro fringes both contribute to the microstructure of a digital hologram, although the latter is the more dominant component. Light grains reflecting off an object's surface are called "specks" because of their erratic nature. Digital holographic interferometry involves the digital capture and approximation of holograms representing the undeformed and deformed states of the object. Based on the method of gathering reference and object beams, two fundamental holographic interferometry layouts are constructed theoretically for capturing the wavefield at the object's surface. The object wave and the reference wave are decoupled in the initial setup by use of wavefront division. Figure 12 shows how this is done by directing the expanded laser beam partially onto the mirror and then onto the object's face.

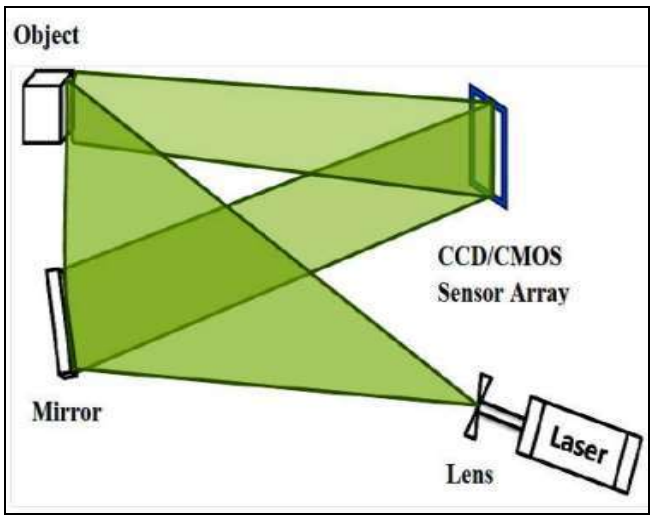

Fig 12: Wave front Division Hologram Construction

Amplitude division hologram construction is the name given to the second arrangement in figure 13. In this configuration, the laser beam is divided into two coherent beams by a beam splitter and then enlarged by a conventional diverging lens. While the other beam immediately reaches the sensor target and creates the reference wave, the first beam lights the item. As a result, the reference wave and object wave are coherently combined, and their interferences are captured in the recording plane.

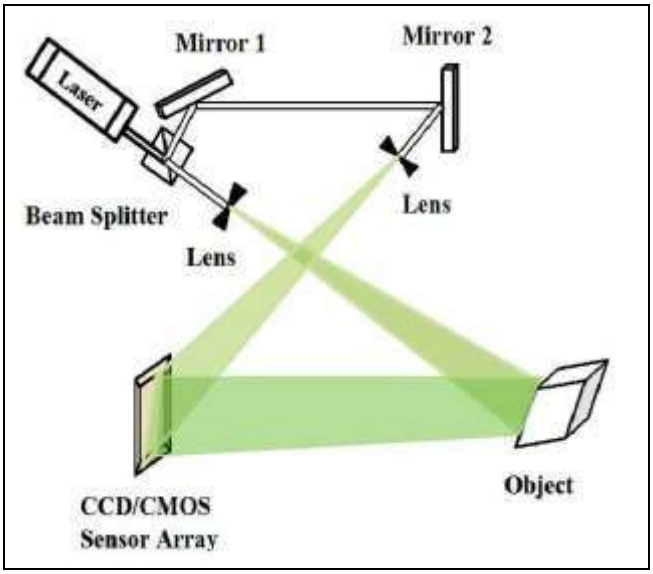

Fig 13: Amplitude Division Hologram Construction

Experimental details

The schematic of holographic interferometry setup used for the static deformation experiment is shown in figure 14.

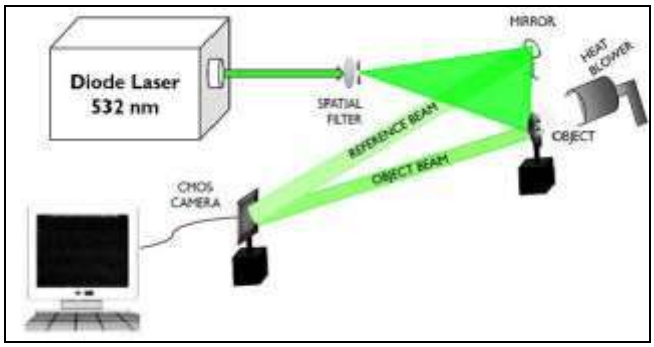

Fig 14: Layout of experimental setup

In this arrangement, a spatial filter assembly is used to expand and filter a narrow laser beam with a long enough coherence length that originates from a 532 nm diode-pumped laser. The main components of the spatial filter assembly are a pinhole and a microscope objective lens. It serves three main purposes. Since the microscope objective used is typically a double concave lens, the first function is to diverge the laser beam. The second function is to remove noise on the holograms caused by dust and scratches on the optics, and the third function is to partially annihilate internal noise created in the laser cavity that travels with the beam. As a consequence, a plane mirror is positioned close by and the filtered beam that results is arranged to fall directly on the item. At the surface of the CMOS sensor, which is the hologram plane, the dispersed waves from the mirror and the object interact with one another. Figure 4.15 depicts the test specimen, a holed metallic tube, which is thermally loaded using a heat blower apparatus.

Fig 15: Snap shot of test specimen

Initial recording of a reference hologram is followed by the continuous recording of succeeding holograms under various static circumstances of the test object. In terms of the phase and amplitude variations brought on by the specimen, it is possible to deduce the modulations of holographic micro fringe patterns that are captured on the CMOS camera. Figure 16 shows a few photos of the holograms that were taken while they were being heated up.

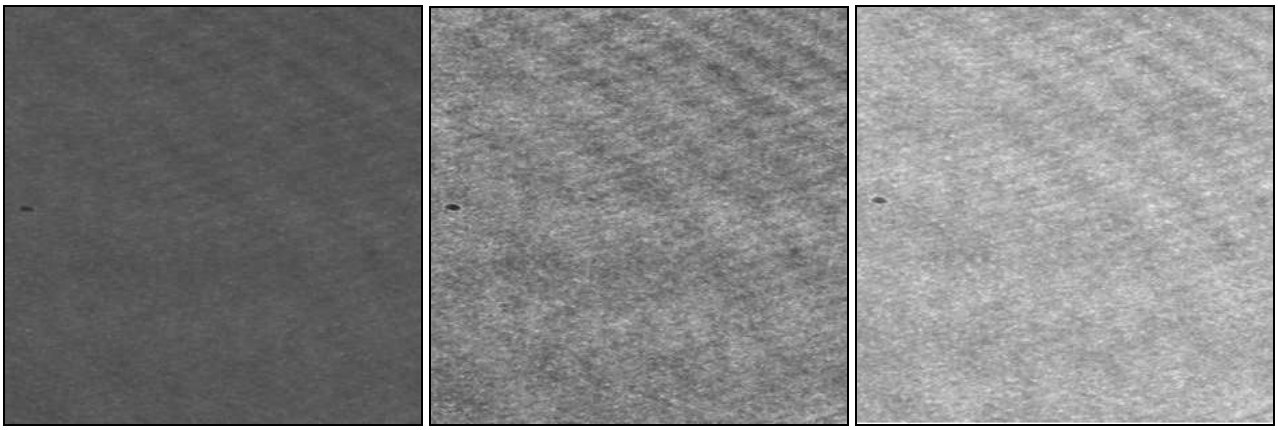

Fig 16: Snap shots of the captured holograms

Using proprietary H-Digital holographic software, it is possible to numerically rebuild double exposure holographic fringe patterns from single exposure holograms. Subtracting the mathematically reconstructed intensities and phases of the undeformed and deformed object wavefronts, respectively, yields the intensity of the double exposure fringe patterns and equivalent interference phase. H Digital© environment shown in figure 17thuseliminates the requirement of a laser for reconstruction of holograms.

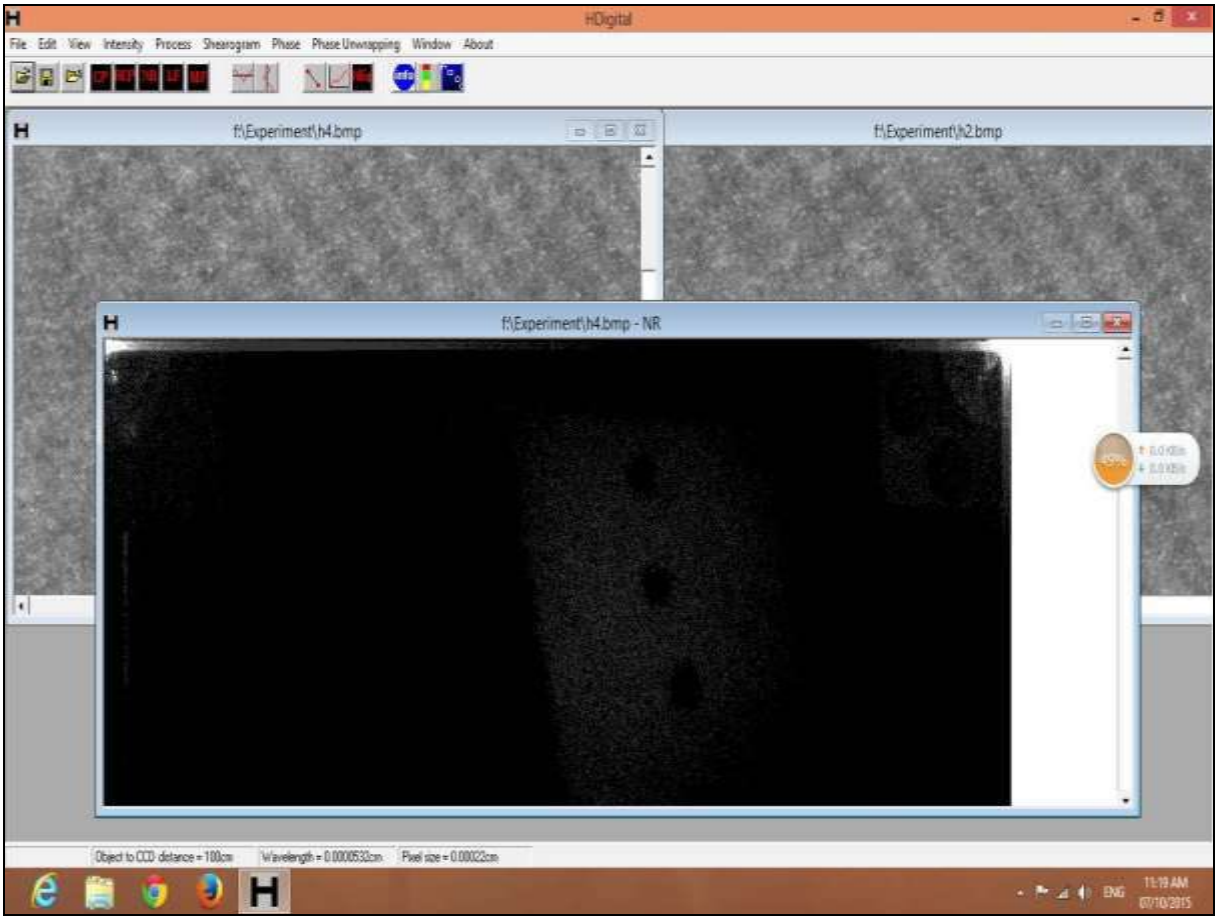

Fig 17: H-Digital © software environment

Results and Discussions

Figure 18 illustrates holographic interference fringes created by numerically reconstructing individual single exposure holograms under two exposures with a reference state. These fringe patterns represent contours of equal displacement brought about by the loading of the item. It is possible to estimate the displacement level to be about equal to $\lambda/2$ from the fringe spacing.

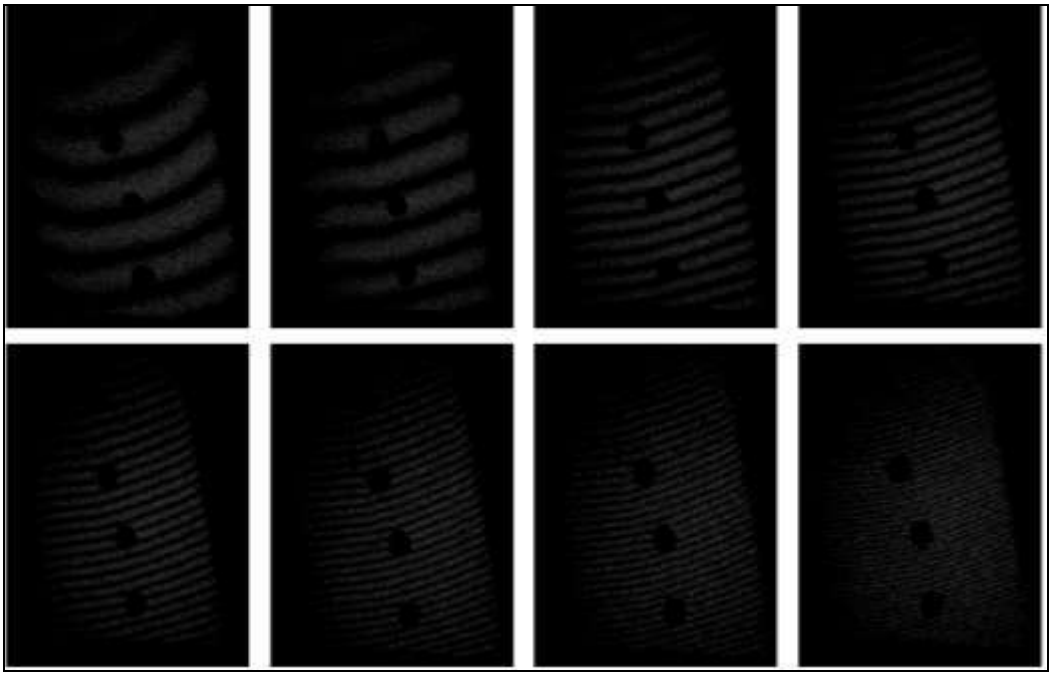

Fig 18: Holographic fringes developed during thermal loading process

The object's imperfection causes regional variations in the surface displacement, which in turn creates fringe anomalies in the normally uniformly fluctuating fringe pattern. The item shape and experimental set-up affect the fringe pattern, which is quite delicate. Thermal deformation phenomena begin to be produced during the heating up process due to

the temperature contrast that has arisen on the specimen's surface. It is understood that when heat is added, the fringe width gets smaller and smaller while the homogeneity is maintained. Since the expansion of the heated specimen has caused thermal deformation, which starts a rise in optical path difference, the thermal loading process results in a larger fringe density. Since the testing temperatures were so low, the outcome clearly shows that the metal tube with holes had been heated evenly and had no flaws noted. Holograms in classical holography cannot be improved once they are recorded and produced, therefore any flaw in the recording process will adversely affect the reconstruction of the hologram. The application of various image processing techniques on digital holograms to optimize the reconstructed pictures allows for the circumvention of this constraint in digital holography. Prior to the double exposure numerical reconstruction, the individual holograms are subjected to the Histogram Equalization (HE) approach to improve the overall brightness and contrast of the restored fringe pattern. The reconstructed picture in figure 19 can be seen to be approximately polluted with noisy flecks, despite the fact that the brightness has been raised overall.

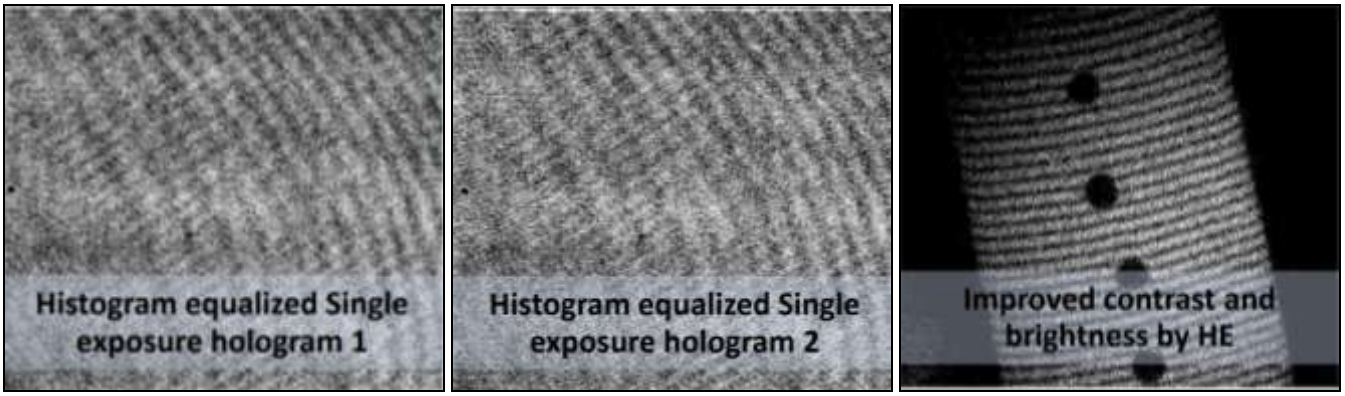

Fig 19: Effect of Histogram Equalization on holographic fringe contrast and brightness

Conclusion

Holographic interferometry, a potent method, is a crucial tool for engineering design, quality control, and non-destructive testing and inspection. In HNDT, a very little stress or excitation is applied to the item being researched, and the behaviour is then observed using HI. The flaws in the item can be identified as a deviation from the normally occurring fringe pattern. HNDT is a whole-field, extremely sensitive, non-contact technology that may be used on objects of any size and form. HNDT can be excited mechanically, thermally, pneumatically, or vibratorily. It was possible to find flaws such inclusions, fractures, voids, debonds, voids, residual stress, improper fittings, and internal abnormalities. HNDT is used to check things like the separation of aviation tyre plies, the delamination of a helicopter rotor blade's composite material, PCB inspection, rocket castings, pressure vessels, and more.

References

1. Blaya Salvador, Carretero Luis, Madrigal RF, Ulibarrena Manuel, Fimia Antonio. New photopolymerizable holographic recording material based on polyvinylalcohol and, 2-hydroxiethylmethacrylate (HEMA). Applied Physics B. 2002;74(6):603-605. 10.1007/s003400200843.
2. Bogodaev N, Ivleva LI, Lykov Pavel, Osiko V, Gordeev A. Dynamic Holography Method for Nondestructive Testing of Optical Homogeneity of Transparent Media. Crystallography Reports. 2010;55(6):1000-1005. 10.1134/S1063774510060167.
3. Brown Matthew, Wright D, M'Saoubi R, McGourly J, Wallis M, Mantle A, *et al*. Destructive and non-destructive testing methods for characterization and detection of machining induced white layer: A review paper. CIRP Journal of Manufacturing Science and Technology, 2018, 23. 10.1016/j.cirpj.2018.10.001.
4. Caulfield H, John YN, Denisyuk, Leith EN. The art and science of holography. A Tribute to Emmett Leith and Yuri Denisyuk; c2003.
5. Caulfield John H, Denisyuk YN, Leith EN. The art and science of holography. A Tribute to Emmett Leith and Yuri Denisyuk; c2003.
6. Cawley Peter. Non-destructive testing - Current capabilities and future directions. Proceedings of The Institution of Mechanical Engineers Part L-journal of Materials-design and Applications - PROC INST MECH ENG L-J Mater. 2001;215(4):213-223. 10.1243/1464420011545058.
7. Charles Vest M. Holographic interferometry, John Wiley and Sons, New York; c1979.
8. Hagemaier DJ. Fundamentals of Eddy Current Testing. American Society for Nondestructive Testing, inc., Columbus, Ohio; c1990.
9. Dai Cuixia, Ying-jie Yu, Chen Gang, Asundi Anand. Study of the holographic phase stitching technique. Proceedings of SPIE - The International Society for Optical Engineering, 2008, 7000. 10.1117/12.783452.
10. Donges Axel, Noll Reinhard. Holographic Interferometry; c2015. 10.1007/978-3-662-43634-9_7.
11. Dwivedi Sandeep, Vishwakarma Manish, Soni Akhilesh. Advances and Researches on Non Destructive Testing: A Review. Materials Today: Proceedings. 2018;5:3690-3698. 10.1016/j.matpr.2017.11.620.
12. Engineering Technologies Division, Nondestructive Testing Development Branch, Chalk River Laboratories, Chalk River, Ontario; c1995.
13. Farahani Mohammadreza, Akbari Davood. Introduction to Nondestructive Testing Methods; c2015.
14. Mayr G, Dietermayr B, *et al*. “Characterization of defects in curved CFRP samples using pulsed thermography and 3D finite element simulation”, 9th

International Conference on Quantitative InfraRed Thermography, Krakow - Poland, July 2008, 2-5.
15. Gandhi Nikita, Rose Rob, Croxford Anthony, Ward Carwyn. Understanding System Complexity in the Non-Destructive Testing of Advanced Composite Products. Journal of Manufacturing and Materials Processing. 2022;6(4):71. 10.3390/jmmp6040071.
16. Ganesan AR. Holographic and laser speckle methods in non-destructive testing. Proceedings of the national seminar and exhibition on non-destructive evaluation. 2009 Vol 5.
17. Ganesan AR. Holographic and laser speckle methods in non-destructive testing. Proceedings of the national seminar and exhibition on non-destructive evaluation. 2009 Vol. 5.
18. García Celia, Fimia Antonio, Pascual Inmaculada. Thick photopolymer layers for holographic recording materials. Proceedings of SPIE - The International Society for Optical Engineering; c2000. 10.1117/12.380017.